Prediction of the fuel spray characteristics in the combustion chamber with methane and TiO2 nanoparticles via numerical modelling

Prediction of the fuel spray characteristics in the combustion chamber with methane and TiO2 nanoparticles via numerical modelling

Dongwei Shao[a], Sami Al Obaid[b], Sulaiman Ali Alharbi[b], Josef Marousek[c,d,e], Manigandan Sekar[f], P. Gunasekar[f], Nguyen Thuy Lan Chi[g,*] Kathirvel Brindhadevi[h], Junfa Wang[a], Donghua Jiang[a,*]

a College of Mechanical Engineering, Jiamusi University, Jiamusi 154007, PR China

b Department of Botany and Microbiology, College of Science, King Saud University, PO Box -2455, Riyadh 11451, Saudi Arabia

c Institute of Technology and Business in České Budejovice, Faculty of Technology, Okružní 517/10, České Budějovice 370 01, Czech Republic

d University of South Bohemia in Ceské Budejovice, Faculty of Agriculture and Technology, Studentská 1668, 370 05 Budějovice, Czech Republic

e Tomas Bata University in Zlín, Faculty of Management and Economics, Mostní 5139, 760 01 Zlín, Czech Republic

f Department of Aeronautical Engineering Sathyabama Institute of Science and Technology, Chennai 600 119, India

g School of Engineering and Technology, Van Lang University, Ho Chi Minh City, Vietnam

h Center for Transdisciplinary Research (CFTR), Department of Pharmacology, Saveetha Dental College, Saveetha Institute of Medical and Technical Sciences, Saveetha University, Chennai, India

** Corresponding authors.*

E-mail addresses: chi.ntl@vlu.edu.vn (N.T.L. Chi), wangcongcong_2004@163.com (D. Jiang).

ABSTRACT

In this study the methane combustion was analysed with the TiO2 nanoparticles. A series of the simulation runs were performed by varying the fuel inlet velocity. However, the oxidizer and the nanoparticles spray were maintained constant for the entire run. The spray velocity varied from 100 m/s to 200 m/s with titanium dioxide (TiO_2) nanoparticles. Using the series of the governing equation and modified Navier Stokes equation the model has been developed with the aid of numerical workbench. Three different domains are generated for fuel, oxidizer and nanoparticles. The velocity of the air and nanoparticles were maintained at constant levels and varying only the spray velocity of the fuel. Based on the findings, the mass fraction of both fuel and formation of the CO2 were dependent on the spray velocity. As the spray velocity increases the turbulence in the combustion chamber increases which ensures the higher mixing of both air-fuel and nanoparticles. From the procured findings 175 m/s and 200 m/s were the ideal range for better combustion efficiency compared to 100 m/s and 150 m/s. The simulation results have ascertained the role of the spray velocity on the emissions and the combustion efficiency of the engine. It is hoped that obtained results can provide directions to work on the combustion of the methane with the nanoparticles at the optimized spray velocity.

1. Introduction

There is a finite supply of petroleum, and it will run out in the near future. Demand for energy has risen dramatically as a result of an increase in the population's growth rate. The fossil fuels extracted from current petroleum reserves contribute significantly to today's energy generation. Because of this, the world's remaining supply of petroleum products like gasoline, diesel, and by-products isn't far away. Fossil fuels used in internal combustion engines, such as aviation fuels, and diesel fuels threatens the environment and affects very badly. In spite of their high efficiency as energy converters, compression ignition engines do environmental harm with their exhaust pollutants **[1-3]**. Heavy-duty diesel engines are the backbone of today' s global transportation industry. For decades, diesel engines have been powered by the usage of conventional diesel fuel. Diesel is the best fuel for compression ignition in diesel engines because of its features. Conventional diesel, on the other hand, has been plagued by a number of problems. There are many dangers to transporting and storing diesel because of its low flash point. Modern diesel engines' exhaust emissions and performance can be improved by switching to alternative fuels or energy sources, therefore this is an urgent necessity.

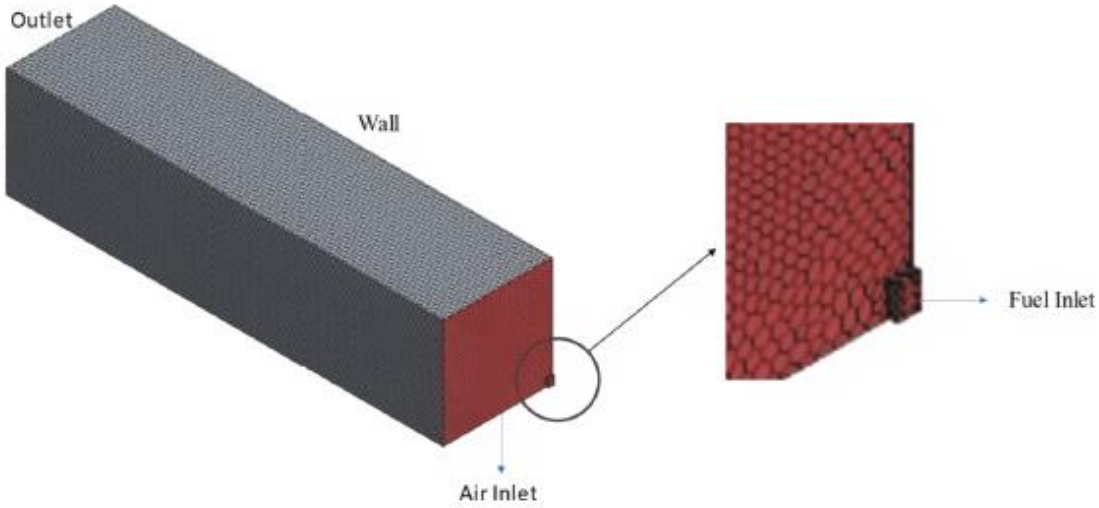

Fig. 1. Meshing model of fuel and air domain.

Table 1 Model settings.

Flow model	Steady- Three dimensional
NOx	Thermal-Zeldovich
Wall treatment	No slip
Fluid	Ideal gas
Enthalpy	Segregated fluid
Flow	Segregated – Turbulent
Species transport	Reacting
Gas component	Multi
Mesh type- Cells- Faces	Multifield reference frame – 64688–443768
Materials properties	Dynamic viscosity
Turbulence model	Standard k-epsilon- SST

Table 2 Species model for the current study.

O_2	0.21
N_2	0.7
Other gas components	0.19
CH_4	0.5
Nanoparticle	0.1% v/v
Injection velocity	100 m/s to 200 m/s
Injector type	Swirl

There are many renewable sources of biofuels, including agricultural feedstocks, organic wastes and algae. Using this green approach can help reduce GHG (Green House Gases) emissions. In addition, biodiesel made from algae produces less GHG emissions **[4-5]**. Because of jatropha's cultivation on wastelands, environmental quality has improved. Potential for jatropha to improve society and the environment has yet to be discovered. It's therefore possible to meet both energy and environmental needs by growing nonedible oilseed crops. As biodiesel's oxygen content rises, the use of alcohols as a biodiesel ingredient becomes more promising . While biodiesel has helped meet the growing demand for alternative fuels, it has shortcomings when it comes to improving the performance of diesel engines and reducing emissions. In the past, researchers have found issues with biodiesel. For biodiesel to have a high brake thermal efficiency, the calorific and energy density must be reduced. Only a few blended samples show a decreasing trend in the concentration of NOx emissions. Biodiesel's high viscosity makes it difficult to atomize and spray, and the combustion process itself produces more pollutants as a result. In addition, biodiesel must be preheated to lower its viscosity before use. Furthermore, the low cold flow qualities of biodiesel make it difficult to carry and store the fuel **[6-7]**. In addition to increasing engine wear, alcohols also have a poor lubricating quality. It burns poorly and causes knocking because of its low cetane number. Alcohol' s energy density is lower than diesels. Furthermore, the blend ability of alcohols

with biodiesel -diesel is slightly lower. Contrary to popular belief, mixing diesel with biodiesel and ethanol has numerous advantages. Lower emissions can be achieved by the use of biodiesel and alcohol because of their increased oxygen content. In contrast to biodiesel, alcohol's viscosity is lower, hence it increases biodiesels. Alcohol and Biodiesel are both biodegradable and clean-burning. Biodiesel and alcohols can be added to diesel because of their accessibility, availability, and affordability. The stability of nanoparticles as a fuel-additive is a major consideration. Because of their vast surface area and activity, nanoparticles prefer to form aggregates. The base fluid's nanoparticle agitation and coagulation can be reduced by adding the correct amount of surfactant. This research suggests that the ideal surfactant for nanoparticles can be selected depending on a number of variables. Biodiesel feedstocks, engine emissions, and performance can all be improved by using biodiesel or nanotechnology, despite the growing number of studies on the subject. The use of different nanoparticles in diesel and biodiesel fuel has been shown to improve the stability, performance, and emissions of the fuel mixes **[8-9]**. In recent days numerical modelling scope has been increased due to the reliability of the numerical results from the user defined simulation. The parameters such as biodiesel blends, fuel atomization' s and emission models were analysed recently using computer simulations **[10-12]**. In this study the methane combustion has been examined along with the 50 ppm of TiO2 nanoparticles. The numerical model had been developed to ensure the combustion performance and emission characteristics (see **Fig. 1**).

2. Numerical simulation

In this study the combustion chamber has been designed with two phase of fluid such as air and methane. The model developed to evaluate the two-phase model via Navier stokes modified equation and large eddy simulations **[12-14]**.

The equation of continuity is

$$\frac{\partial u}{\partial x}+\frac{\partial v}{\partial y}=0 \tag{1}$$

Equations of momentum **[8]** are

$$\rho\frac{\partial u}{\partial t}=-\frac{\partial p}{\partial x}+\mu\left(\frac{\partial^2 u}{\partial x^2}+\frac{\partial^2 u}{\partial y^2}\right)-\sigma_e {B_0}^2 u\sin^2\alpha \tag{2}$$

$$\rho\frac{\partial v}{\partial t}=-\frac{\partial p}{\partial y}+\mu\left(\frac{\partial^2 v}{\partial x^2}+\frac{\partial^2 v}{\partial y^2}\right) \tag{3}$$

Equation of state of the developed model is based on the Matheis et al., (2018) and Xia et al., (2021) **[15,11]**.

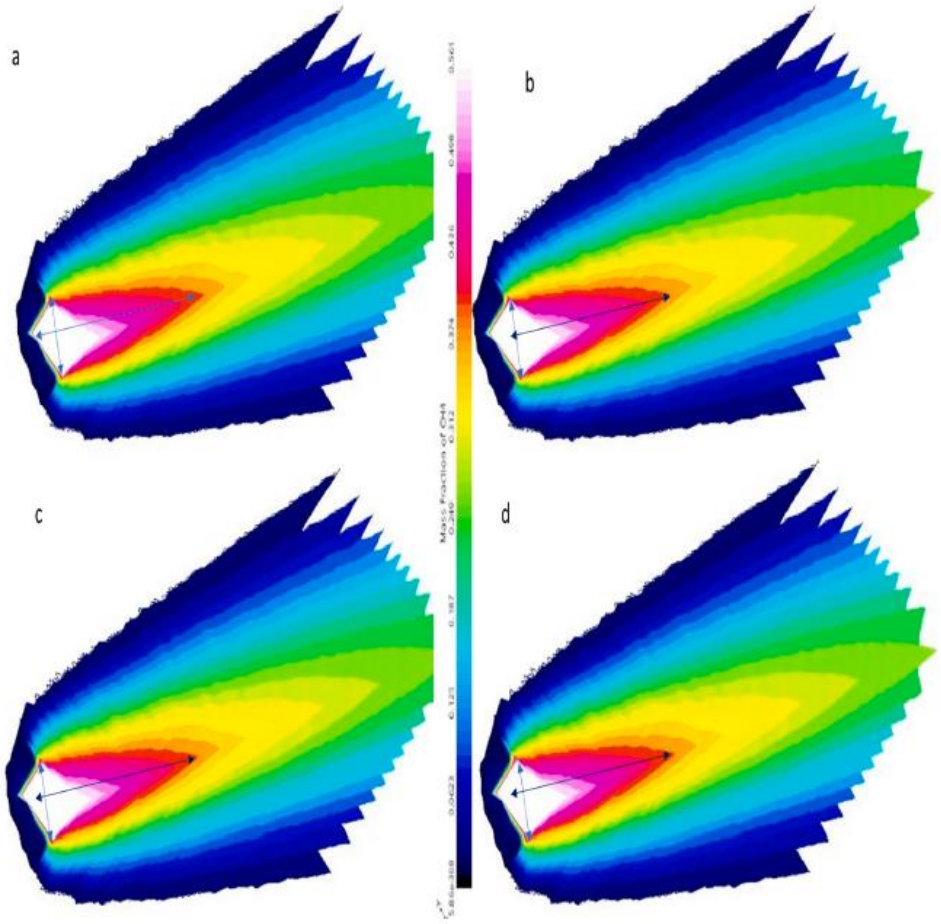

Fig. 2. Mass fraction of CH_4 at various injection velocities a) 100 m/s b) 150 m/s c) 175 m/s d) 200 m/s.

Navier strokes equation in fully conservative function Huazhou Li (2022) **[16],**

$$\partial_t E + \nabla.[(E+p)\boldsymbol{u}] = \nabla.(\boldsymbol{u}.\boldsymbol{\tau} - \boldsymbol{q}) \tag{4}$$

Pressure evolution equation,

$$\partial_t p + \nabla.(p\boldsymbol{u}) = \left(p - \rho c^2\right)\nabla.\boldsymbol{u} \cdots + \frac{\alpha_p}{c_v \beta_T \rho}[\nabla.(\boldsymbol{\tau}.\boldsymbol{u} - \boldsymbol{q}) - \boldsymbol{u}.(\nabla.\boldsymbol{\tau})] \cdots +$$

$$\sum_{i=1}^{N_c} \frac{1}{\rho}\frac{\partial p}{\partial Y_i}\Big|_{\rho,\epsilon,Y_{j\neq i}} \nabla \boldsymbol{J}_i \tag{5}$$

The above equation **(5)** has been modified from the fully conservative function. The state vector consists of ρ- mass density, partial densities ρY_i of species $i = \{1 \ldots N_c\}$, c - speed of sound, c_v-heat capacity at constant volume, and α_p - thermal expansion and β_T- Isothermal compressibility coefficient and $\rho\mathbf{u}$- linear momentum **[15]**.

Total energy density,

$$E = \rho e + \frac{1}{2}\rho \boldsymbol{u}.\boldsymbol{u}(\mathrm{PC}) \tag{6}$$

Velocity vector in a Cartesian frame of reference

$$\text{Pressure } p(\mathrm{QC}).\boldsymbol{u} = \left[u_1, u_2, u_3\right]^T \tag{7}$$

Equation of state for the multiphase problem given by,

$$p\left(v\_, T, \boldsymbol{z}\right) = \frac{\mathscr{R}T}{v\_ - b} - \frac{a\alpha}{v\_^2 + ubv\_ + wb^2} \tag{8}$$

p- Pressure; *v*- function of the molar volume, T- temperature and z-molar composition, where $z = \{z, \ldots, z_{N_i}\}$. $\mathcal{R}$-universal gas constant. The function is based on the Peng and Robinson (1976) **[16,17]**.

$$\alpha = \left[1 + c_0\left(1 - \sqrt{T_{red}}\right)\right]^2 \; with \; T_{red} = T/T_c \tag{9}$$

Accounts for the polarity of a fluid and is a correlation of temperature T, critical temperature T_c and acentric factor ω

$$c_0 = 0.37464 + 1.5422\omega - 0.2699\omega^2 \tag{10}$$

T_{red} = T/T_c is known as the reduced temperature. The parameter a = $0.45724(\mathcal{R}^2T_c^2/p_c\}$ represents attractive forces between molecules and the effective molecular volume is represented by.b = $0.0778(\mathcal{R}T_c/p_c)$ The parameters required in the EOS are calculated from Reid et al. (1987) **[18,19]**.

$$a\alpha = \sum_{i}^{N_c}\sum_{j}^{N_c} z_i z_j a_{ij}\alpha_{ij} \text{and} b = \sum_{i}^{N_c} z_i b_i \qquad (11)$$

with z_i being the mole fraction of component i(overall or in the liquid/ vapor phase).

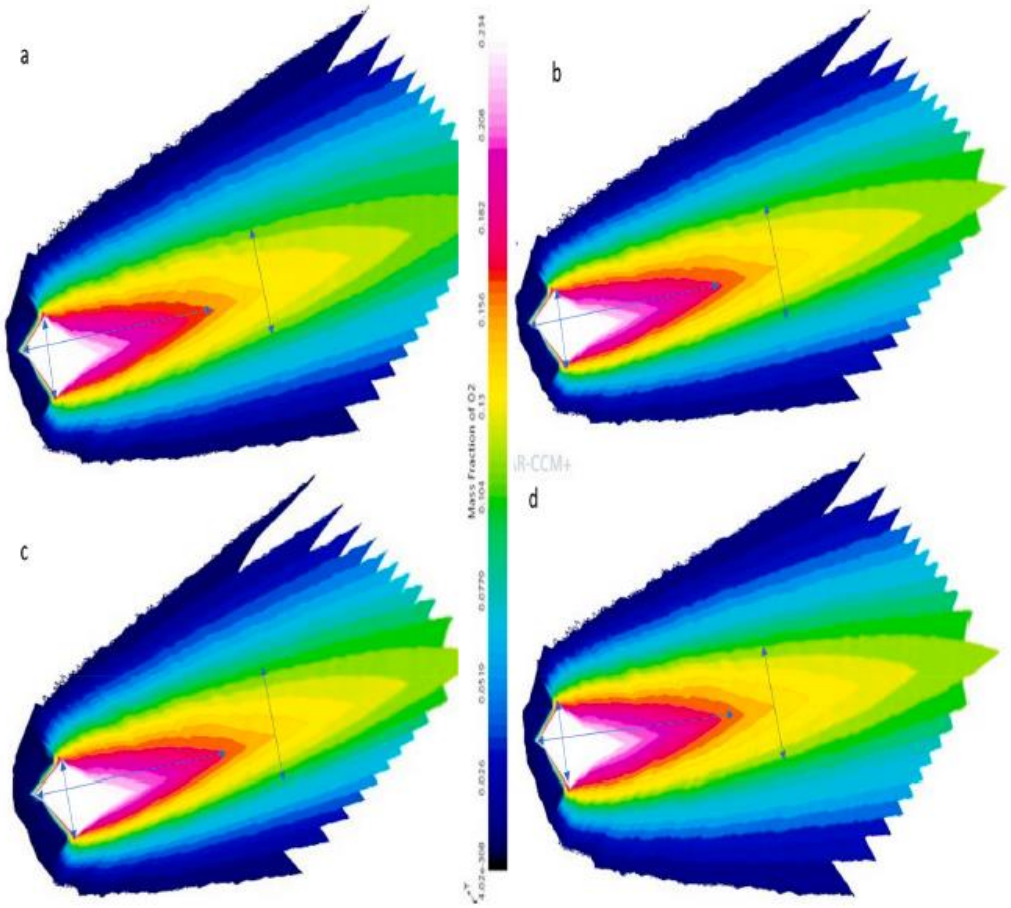

Fig. 3. Mass fraction of O_2 at various injection velocities a) 100 m/s b) 150 m/s c) 175 m/s d) 200 m/s.

2.1. Simulation model

In this study, the STAR CCM + simulation tool has been utilized to analyse the importance of the methane and air combustion. The combustion chamber has been designed as the axisymmetric model. Two inlets have been designed to allow air and methane. Each fluid has passed at different velocities to ensure proper mixing in the combustion chamber. To observe the effects of fuel spray velocity four

variation studies had been done by varying the inlet velocity of methane from 100 m/s to 200 m/s in the intervals of 25 m/s. However, the ambient velocity said to maintained constant at 2 m/s. Although the ambient air is laminar, the methane passed at turbulent state to ensure proper mixing in the combustion chamber. Air domain was defined with inlet velocity and outlet atmosphere opening and the same used for the fuel inlet as well. Ensuring good mixing ratio leads to better combustion efficiency. Standard k-epsilon turbulence model has been used to analyse the thermodynamic model which contains five different species. All the cases were solved at the steady state conditions. Here, there are four different domains such as air inlet, fuel inlet, wall and nanoparticle inlet. The nanoparticles were supplied in the fuel domain in the volume basis. The wall used here is no slip wall with no heat transfer rates. All domains are meshed in the structured sizing. The total number of nodes and elements were 32,261 and 32,000 respectively. Post solver were used to develop the interaction between the mesh model and the output solution **[20-21]**. **Table 1** shows the model settings for the current analysis. Further, the **Table 2** provides the details of the flow properties used in the current study.

3. Results and discussion

A series of test conducted by varying the fuel inlet velocities 100 m/s, 150 m/s, 175 m/s and 200 m/s. The parameters such as CH4, O2, NO, and turbulence intensity were captured for all velocities and compared to one another.

3.1. Mass fraction of CH4

Fig. 2 represents the distribution of the CH_4 in the combustion chamber at the various fuel injection velocities of 100 m/s, 150 m/s, 175 m/s and 200 m/s using an iso-surface model. From the comparative representation it is clear that the velocity does not play the major role in the burning of the CH_4. In all cases, the starting point of the burning is identical. Nevertheless, the extension of the combustion core length is higher when the velocity of the injection has been increased. When the injection velocity is increased, the spray characteristics have been changed which effectively enhanced the distribution of fuel in the entire combustion chamber. At 100 m/s, the distribution length is smaller compared to the 200 m/s of injection velocity. Which is clearly represented by showing the double arrow heads in the combustion chamber.

By comparing all the velocities, the 150 m/s and 175 m/s reported higher core length than 100 m/s and 200 m/s. When the velocity increased beyond 175 m/s, the combustion flame length was reduced. Higher the flame length larger the turbulence intensity in the combustion chamber. When the turbulence intensity has been increased the possibility of having complete combustion was high **[22,23]**. Although the intensity of the CH_4 for each case varies, they are mostly identical when the combustion zone reaches a fully expanded state as depicted in the figures owing to the presence of TiO2 in the combustion chamber. Irrespective of the injection velocity, the CH_4 variation at the exit is similar to one another. The maximum mass fraction of 0.561 CH_4 has been observed at the lip of the combustion chamber due to the premixing of the air and fuel.

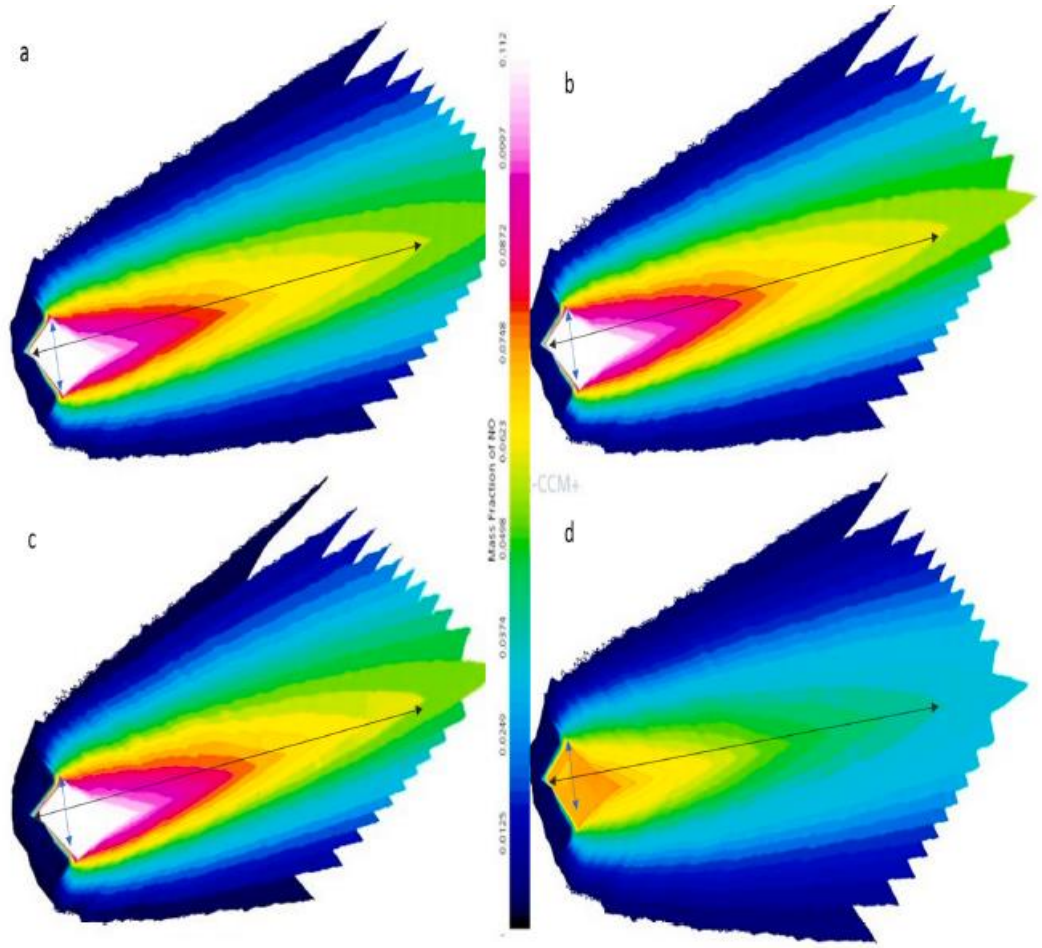

Fig. 4. Mass fraction of NO at various injection velocities a) 100 m/s b) 150 m/s c) 175 m/s d) 200 m/s.

3.2. Mass fraction of O_2

In order to understand the nature of the combustion, **Fig. 3** represents the mass fraction of the oxygen molecules. There is no significant change in the O_2 has been observed for all cases. On the other hand, the core length of the O_2 distribution was reduced when the injection velocity of the fuel exceeded 175 m/s. **Fig. 2 and Fig. 3** are identical since the rate of combustion depends on the Air-Fuel ratio. There is no evidence of the change in the vertical height of the diamond wedge which is mainly due to the constant air speed and excess of oxygen atoms due to the addition of nanoparticles. In the current study, the air velocity is subjected to be constant irrespective of the different fuel injection velocities. As the length of the combustion chamber increases the distribution of the O_2 is reduced which denotes the complete combustion. At the tip of the combustion chamber the presence of the oxygen molecules was nearly zero. This typically denotes the effective mixing of the air and fuel **[24]**. Compared to all velocities, 200 m/s injection velocity marginally performed higher than other velocities by clocking higher combustion. Although there is no evidence of the change in the combustion core along the horizontal axis, some marginal change has been observed at the vertical axis as represented using the convention line techniques represented in the figure.

3.3. Mass fraction of NO emission

Typically, the concentration of the nitrogen was higher in the air species. During the combustion of any fuel products emit higher rates of nitrogen or oxides. Among different greenhouse gases, the emission of NOx was a big concern to reduce the impact of the fuels on the environment **[25,26]**. The possibility of the reduction of the NOx in the exhaust is not possible. However, the concentration of NOx can be reduced by using the green fuels such as hydrogen, methane and biodiesel. On the other hand, attaining the complete combustion in the inside the chamber also leads to reduced formation of NO. **Fig. 4** shows the distribution of mass fraction of NO at different injection velocities. In this case, the use of the CH_4 as the fuel reduced the formation of the NO.

During the process of combustion, the presence of the nitrogen is high at the tip of the combustion chamber. As the combustion chamber length increased, the formation of the nitrogen has been decreased drastically owing to the complete combustion. With regard to the injection velocities, there is no evidence of change in the NO for the velocities such as 100 m/s, 150 m/s and 175 m/s. However, once the injection velocity increased beyond 175 m/s, there is evidence of drastic reduction in the NO formation in the combustion chamber. This depicts that, increasing the fuel spray velocities plays the major role in achieving higher combustion which leads to lower formation of exhaust pollutants [27,30]. To be very precise, the maximum NO obtained at the velocities such as 100 m/s, 150 m/s, 175 m/s and 200 m/s are 0.12, 0.097, 0.095 and 0.0748 respectively.

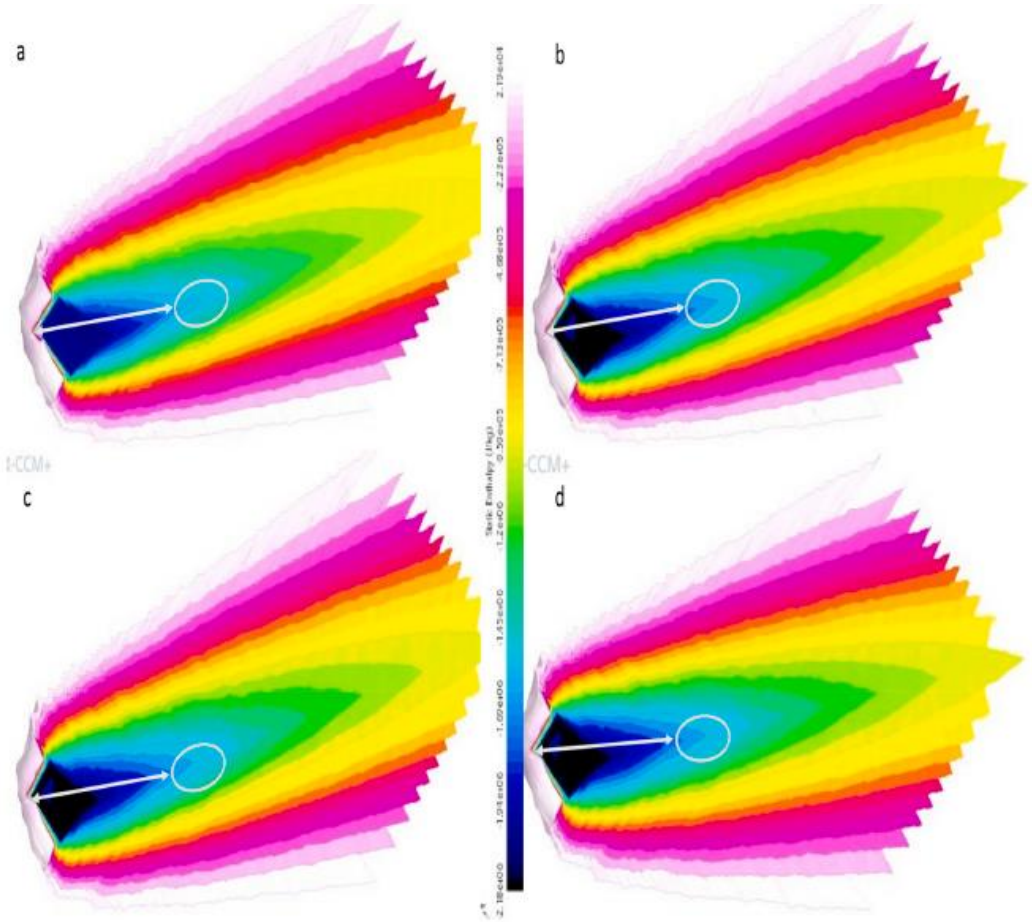

Fig.5 Mass fraction of static enthalpy at various injection velocities a) 100 m/s b) 150 m/s c) 175m/s d) 200 m/s

Fig. 5 represents change in the static enthalpy of the system. In general, enthalpy of combustion is used to calculate the intensity of the energy released when 1 mol of the CH_4 has been burnt at standard conditions **[28]**. There is no evidence of change in the static enthalpy when the injection velocity of the fuel was increased. All the cases reported the same rate of static enthalpy. The maximum static enthalpy reported by the 100 m/s, 150 m/s, 175 m/s and 200 m/s were 1.94e6 J/ kg and the minimum has been reported on the combustion chamber walls. Although there is no evidence of the significant change in the static enthalpy at the combustion stage, there is a slight change in the increase of the static enthalpy at the mid portion of the combustion chamber where the combustion is reaching fully developed stage. As the velocity of the fuel injection increased there is slight change in the enthalpy has been reported at higher injection velocity which is greater than 150 m/s. As the injection velocity increased the rate of the combustion was increased which leads to higher static enthalpy.

3.4. Enthalpy of combustion

Fig. 5 represents change in the static enthalpy of the system. In general, enthalpy of combustion is used to calculate the intensity of the energy released when 1 mol of the CH4 has been burnt at standard conditions **[28]**. There is no evidence of change in the static enthalpy when the injection velocity of the fuel was increased. All the cases reported the same rate of static enthalpy. The maximum static enthalpy reported by the 100 m/s, 150 m/s, 175 m/s and 200 m/s were 1.94e6 J/ kg and the minimum has been reported on the combustion chamber walls.

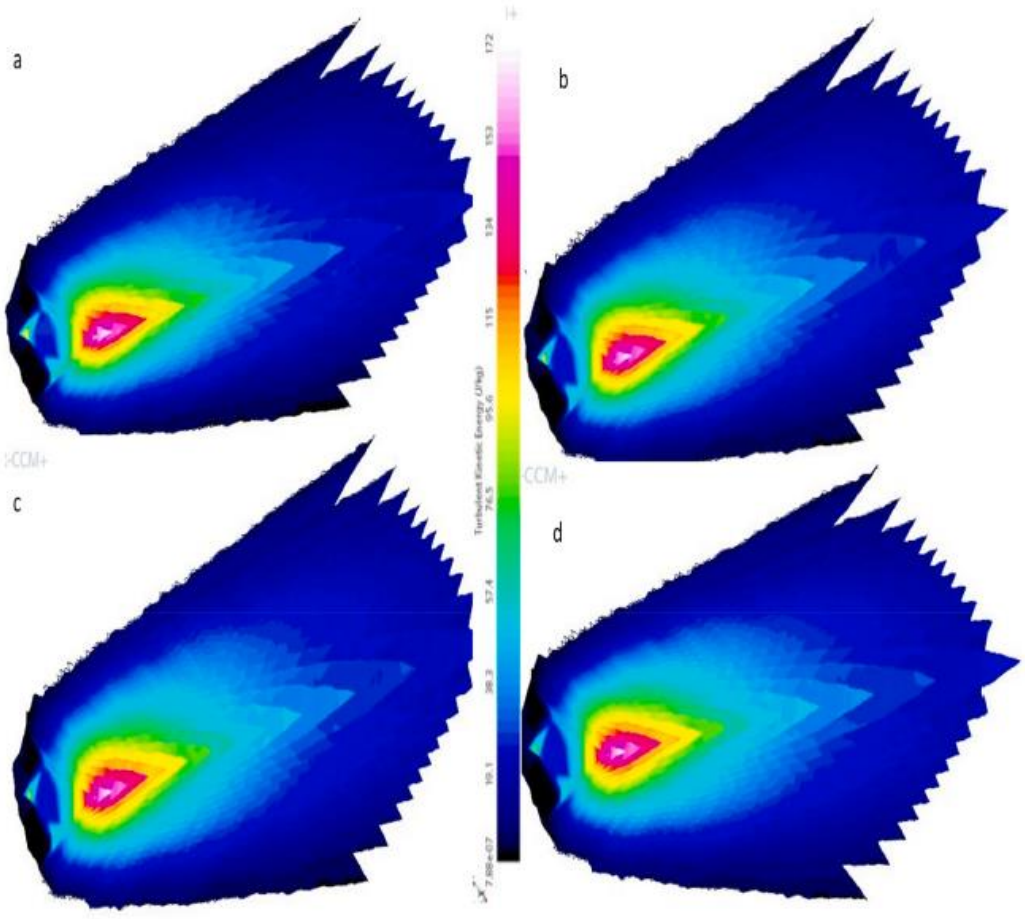

Fig. 6. Change in the turbulent kinetic energy at various injection velocities a) 100 m/s b) 150 m/s c) 175 m/s d) 200 m/s.

Although there is no evidence of the significant change in the static enthalpy at the combustion stage, there is a slight change in the increase of the static enthalpy at the mid portion of the combustion chamber where the combustion is reaching fully developed stage. As the velocity of the fuel injection increased there is slight change in the enthalpy has been reported at higher injection velocity which is greater than 150 m/s. As the injection velocity increased the rate of the combustion was increased which leads to higher static enthalpy.

3.5. Effect of flow turbulence on combustion

The turbulent kinetic energy is another way to measure the effectiveness of the combustion efficiency. When the fuel and air mixed at higher turbulence ratio there was an increase in the vaporization of the fuel. Further, the atomization of the fuel was also increased when the turbulence intensity inside the combustion chamber has been enhanced **[11]**. In order to ensure higher turbulence in the combustion chamber, the fuel was sprayed using the swirl vanes. Using the swirl vanes enhances the turbulence and makes sure the Fuel-Air mixes properly. **Fig. 6** represents the turbulent kinetic energy for various inlet fuel spray velocities. The maximum turbulence has been noticed at the point were the concentration of the CH_4 is higher. As the length of the combustion chamber increased there was a reduction in the kinetic energy. At the fully developed region the total kinetic energy presence is negligible. With regard to the velocities, 200 m/s witnessed higher turbulence than other injection velocities. In the current study, the inlet velocity of the air is constant, however there is a change in the injection velocity of fuel. Hence the fuel plays the major role in increasing the turbulence inside the combustion chamber. When the fuel is injected at higher velocity, high turbulence has been created inside the combustion chamber which leads to higher rates of combustion and lower formation of NO pollutants **[29]**. From the previous figures it is clear the role of the turbulence on the efficiency of the combustion chamber and exhaust emissions were immense. In order to prove the role of turbulence in the combustion chamber the turbulent viscosity ratio has been measured for all cases. **Fig. 7** showcases the change in the turbulence viscosity ratio for various fuel injection velocities. From the figure it is well clear that the rate of turbulence viscosity ratio was higher at 100 m/s compared to other cases. At lower injection velocities there is a slight increase in the combustion duration. Hence compared to all cases, 100 m/s showed a higher viscosity ratio. From the above it is understood that turbulence kinetic energy and turbulent viscosity ratio were opposite to one another. Larger the viscosity lowers the turbulence energy.

3.6. Effect of vorticity on the injection velocity

Unlike the turbulence viscosity ratio and turbulence kinetic energy, the vorticity plays the crucial role in determining the effectiveness of the combustion. Higher formation of the vortices in the combustion chamber depicts profound change in the overall combustion. **Fig. 8** shows the distribution of the vortices inside the combustion chamber **[11]**. From the previous findings it is clear that the majority of the combustion takes place near the tip of the combustion chamber and the combustion energy dissipates as the length of the combustion chamber increases. The current vorticity images also represent the same. Similar to above, the maximum vortices have been formed at the initial part of the combustion and the energy of the vortices dissipates when the flow attains the region of fully developed.

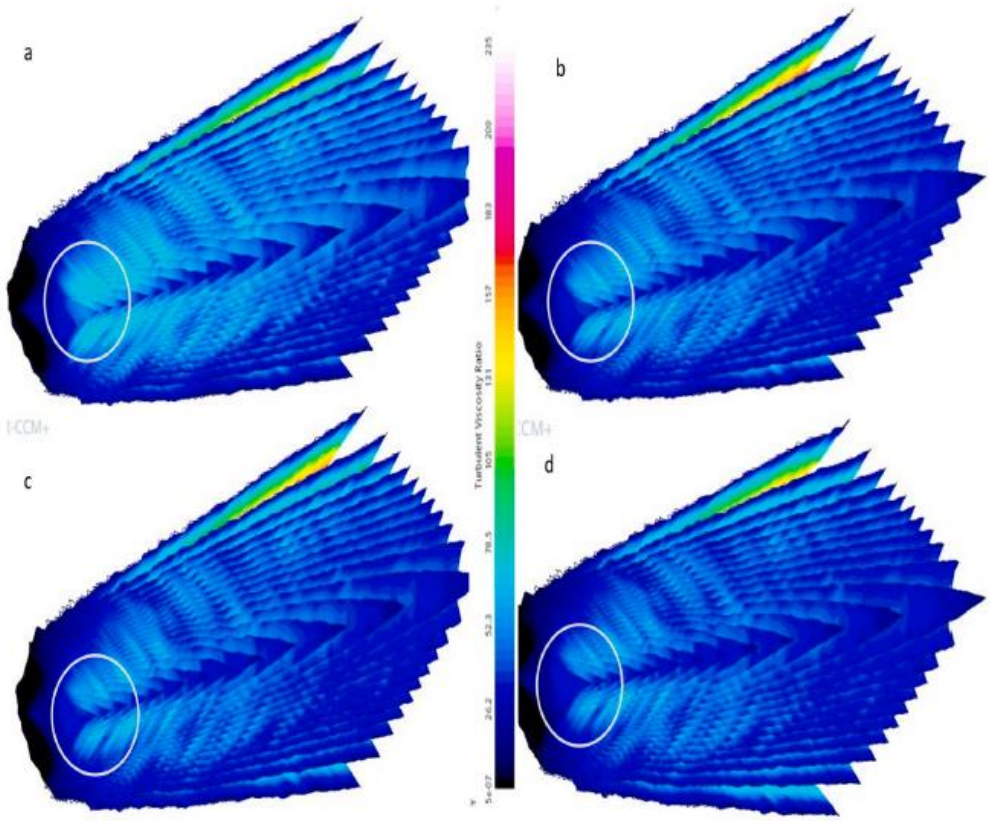

Fig. 7. Change in the turbulent viscosity ratio at various injection velocities a) 100 m/s b) 150 m/s c) 175 m/s d) 200 m/s.

However, there has been evidence of change in the vortices with respect to the change in injection velocity. At 100 m/ s, the intensity of the vortices were not very high enough like other cases. The formation of the diamond wedge on the 150 m/s to 200 m/s injection velocity is higher than 100 m/s. This clearly shows the role of injection velocity on the formation and distribution of the vortices **[29]**. From the above it is clear that vorticity plays an important role in enhancing the combustion performance of the engine. **Fig. 9** shows the in-plane spectral contours of the change in the mass fraction of both fuel and air. In addition to above, the distribution of the turbulence energy was also examined.

4. Conclusion

In the current study, the influence of the fuel injection velocity on the combustion efficiency has been examined. In order to understand the effectiveness of combustion the parameters such as mass fraction, turbulence intensity and static enthalpy of combustion were examined at four different fuel inlet velocities such as 100 m/s, 150 m/s, 175 m/s and 200 m/s. Change of velocity does not create a major difference in the magnitude of the fuel mass fraction. However, the length of the flame is higher when the injection velocity is high. Compared to all the

velocities, 175 m/s flame length is longer with better stability. However, based on the concentration of the oxygen atom's presence, 200 m/s injection velocity inches marginally higher than 175 m/s which is viable by obtaining higher combustion efficiency. When the velocity of fuel injection increases the rate of combustion increases. Nevertheless, the influence of the nanoparticles on the combustion

reaction were also enormous. With regard to the emission of the NO, the 200 m/s injection velocity reported 46%, 34% and 25% lesser emissions than other injection velocities. Further, increasing the velocity affects the stagnation enthalpy of the combustion positively. On the other hand, at the higher velocities, the turbulent kinetic energy was also increased due to the lower turbulent viscosity ratio and high vortices. From the above it is clear that, in order to achieve the enhanced combustion, the optimization of the fuel injection velocity is crucial. By varying the fuel injection velocity one can alter the performance of the engine by augmenting the turbulence intensity in the combustion chamber. The predicted model can be used in future for a wide range of test blends.

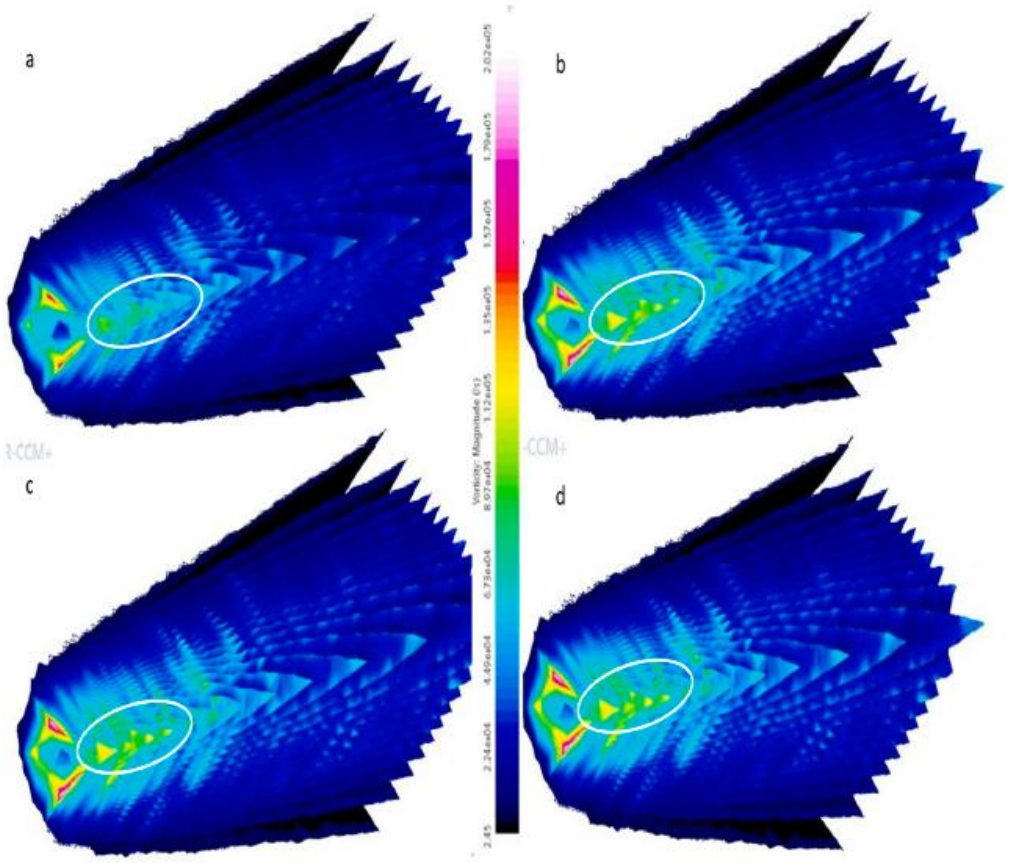

Fig. 8. Change in the vortices at various injection velocities a) 100 m/s b) 150 m/s c) 175 m/s d) 200 m/s.

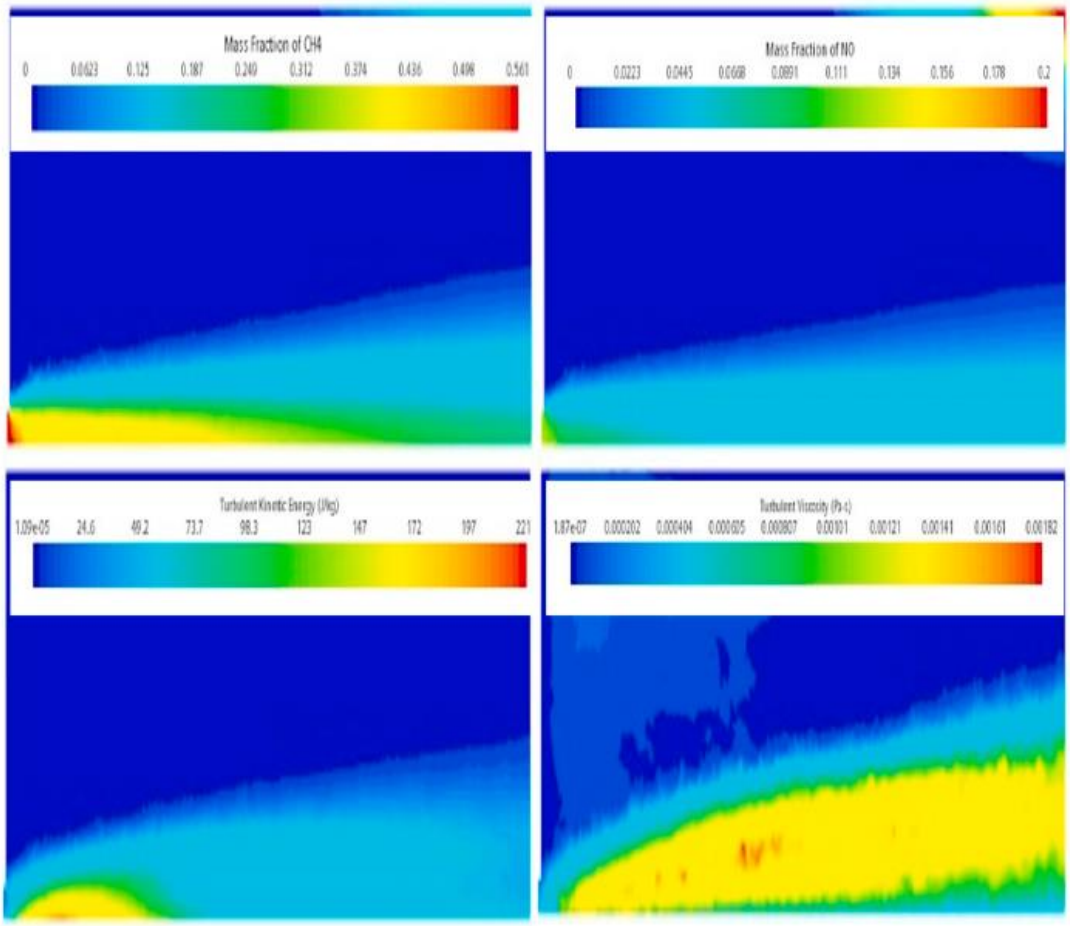

Fig. 9. In-plane spectral distribution for various contours at 200 m/s.

References

[1] Anderson A, Al-Mohaimeed AM, Elshikh MS, Praveenkumar TR, Sekar M. Exergy and energy analysis of a-Fe2O3-Doped Al2O3 nanocatalyst-based biodiesel blends—performance and emission characteristics. J Energy Res Technol 2021;143 (12):1-32.

[2] Sekar M, Ponnusamy VK, Pugazhendhi A, Nizetic S, Praveenkumar TR. Production and utilization of pyrolysis oil from solidplastic wastes: A review on pyrolysis process and influence of reactors design. J Environ Manage 2022;302:114046.

[3] Salam S, Choudhary T, Pugazhendhi A, Verma TN, Sharma A. A review on recent progress in computational and empirical studies of compression ignition internal combustion engine. Fuel 2020;279:118469. https://doi.org/10.1016/j. fuel.2020.118469.

[4] Orejuela-Escobar LM, Landazuri AC, Goodell B. Second generation biorefining in Ecuador: Circular bioeconomy, zero waste technology, environment and sustainable development: The nexus. J Bioresour Bioprod 2021;6:83-107.

[5] Al-Kheraif AA, Syed A, Elgorban AM, Divakar DD, Shanmuganathan R, Brindhadevi K. Experimental assessment of performance, combustion and emission characteristics of diesel engine fuelled by combined non-edible blends with nanoparticles. Fuel 2021;295:120590.

[6] Xia C, Brindhadevi K, Elfasakhany A, Alsehli M, Tola S. Performance, combustion and emission analysis of castor oil biodiesel blends enriched with nanoadditives and hydrogen fuel using CI engine. Fuel 2021;306:121541.

[7] Ge S, Brindhadevi K, Xia C, Elesawy BH, Elfasakhany A, Unpaprom Y, et al. Egg shell catalyst and chicken waste biodiesel blends for improved performance, combustion and emission characteristics. Fuel 2021;306:121633.

[8] Rana A, Sudhaik A, Raizada P, Nguyen V-H, Xia C, Khan AAP, et al. Graphitic carbon nitride based immobilized and non-immobilized floating photocatalysts for environmental remediation. Chemosphere 2022;297:134229.

[9] Ganesan R, Narasimhalu P, Joice Joseph AI, Pugazhendhi A. Synthesis of silver nanoparticle from X-ray film and its application in production of biofuel from jatropha oil. Int J Energy Res 2020:1-11. https://doi.org/10.1002/er.6106.

[10] Al-Dawody MF, Edam MS. Experimental and numerical investigation of adding castor methyl ester and alumina nanoparticles on performance and emissions of a diesel engine. Fuel 2022;307:121784.

[11] Xia C, Brindhadevi K, Elfasakhany A, Alsehli M, Tola S. Numerical modelling of the premixed compression ignition engine for superior combustion and emission characteristics. Fuel 2021;306:121540.

[12] Liu A, Gao Z, Rigopoulos S, Luo KH, Zhu L. Modelling of laminar diffusion flames with biodiesel blends and soot formation. Fuel 2022;317:122897.

[13] Subramani N, Kengaiah SMV, Prakash S. Numerical modeling on dynamics of droplet in aircraft wing structure at different velocities. Aircraft Eng Aerospace Technol 2022;94(4):553-8.

[14] Wu Y, Altuner EE, Tiri RNEH, Bekmezci M, Gulbagca F, Aygun A, et al. Hydrogen generation from methanolysis of sodium borohydride using waste coffee oil modified zinc oxide nanoparticles and their photocatalytic activities. Int J Hydrogen Energy 2022. https://doi.org/10.1016/j.ijhydene.2022.04.177.

[15] Matheis J, Hickel S. Multi-component vapor-liquid equilibrium model for LES of high-pressure fuel injection and application to ECN Spray A. Int J Multiph Flow 2018;99:294-311.

[16] Li H. Multiphase Equilibrium Calculations. InMultiphase Equilibria of Complex Reservoir Fluids 2022 (pp. 163-210). Springer, Cham.

[17] Peng DY, Robinson DB. A new two-constant equation of state. Ind Eng Chem Fundam 1976;15(1):59-64.

[18] Román-Ramírez LA, Leeke GA. Evaluation of the Peng-Robinson and the cubic-plus-association equations of state in modeling VLE of carboxylic acids with water. Int J Thermophys 2020;41(5):1-27.

[19] Reid, RC, Prausnitz, JM, and Poling, BE. The properties of gases and liquids. United States: N. p., 1987. Web.

[20] Pichaimuthu C, Swaminathan G. Rotating flow thorough parallel plates with the various inclined magnetic field under the influence of hall current. Aircraft Eng Aerospace Technol 2022;94(4):564-9.

[21] Wang Y, Wang P. Numerical investigation on the n-heptane spray flame at hydrous ethanol premixed condition. J Energy Res Technol 2022;144(10):102301.

[22] Mikulčic H, Baleta J, Wang X, Wang J, Qi F, Wang F. Numerical simulation of ammonia/methane/air combustion using reduced chemical kinetics models. Int J Hydrogen Energy 2021;46(45):23548-63.

[23] Nonaka HO, Pereira FM. Experimental and numerical study of CO2 content effects on the laminar burning velocity of biogas. Fuel 2016;182:382-90.

[24] Fordoei EE, Mazaheri K, Mohammadpour A. Numerical study on the heat transfer characteristics, flame structure, and pollutants emission in the MILD methane-air, oxygen-enriched and oxy-methane combustion. Energy 2021;218:119524.

[25] Sangeetha M, Boomadevi P, Khalifa AS, Brindhadevi K, Sekar M. Vibration, acoustic and emission characteristics of the chlorella vulgaris microalgae oil in compression ignition engine to mitigate environmental pollution. Chemosphere 2022;293:133475.

[26] Li X, Zhen X, Xu S, Wang Y, Liu D, Tian Z. Numerical comparative study on knocking combustion of high compression ratio spark ignition engine fueled with methanol, ethanol and methane based on detailed chemical kinetics. Fuel 2021; 306:121615.

[27] Akbarian E, Najafi B, Jafari M, Faizollahzadeh Ardabili S, Shamshirband S, Chau KW. Experimental and computational fluid dynamics-based numerical simulation of using natural gas in a dual-fueled diesel engine. Eng Appl Comput Fluid Mech 2018;12(1):517-34.

[28] Zhou C, Tang A, Cai T, Zhao D, Huang Q. Numerical study on flame shape transition and structure characteristic of premixed CH4/H2-air in the micro-planar combustor. Chem Eng Process Process Intensification 2021;166:108460.

[29] Gopal A, Dhavare P, Ali Alharbi S, Nasif O, Strunecký O, Nithya S. Effect of injection pressure on spray cone and penetration angle for enhancedfuel atomization of various blended viscous fluid: A numerical modelling. J Energy Res Technol 2022;13:1-7.

[30] Gao J, Xing S, Tian G, Ma C, Zhao M, Jenner P. Numerical simulation on the combustion and NOx emission characteristics of a turbocharged opposed rotary piston engine fuelled with hydrogen under wide open throttle conditions. Fuel 2021;285:119210.